



Research article

Facile coating of urinary catheter with bio-inspired antibacterial coating

Mohamed A. Yassin^{a,b,*}, Tarek A. Elkhooly^c, Shereen M. Elsherbiny^d, Fikry M. Reicha^d, Ahmed A. Shokeir^e^a Packaging Materials Department, National Research Centre, Giza, Egypt^b Advanced Materials and Nanotechnology Lab., Center of Excellence, National Research Centre, Giza, Egypt^c Refractories, Ceramics and Building Materials Department, National Research Centre, Giza, Egypt^d Biological Advanced Materials, Physics Department, Faculty of Science, Mansoura University, Mansoura, Egypt^e Center of Excellence of Genome and Cancer Research, Urology and Nephrology Center, Mansoura University, Mansoura, Egypt

ARTICLE INFO

Keywords:

Materials science
Nanomaterials
Coatings
Materials characterization
Supramolecular chemistry
Urology
Urinary catheters
Polydopamine
Silver nanoparticle
Antibacterial
Antifouling

ABSTRACT

Formation of bacterial biofilm on indwelling urinary catheters usually causes catheter-associated urinary tract infections (CAUTIs) that represent high percent of nosocomial infections worldwide. Therefore, coating urinary catheter with antibacterial and antifouling coating using facile technique is in great demand. In this study, commercial urinary catheter was coated with a layer of the self-polymerized polydopamine which acts as active platform for the in situ formation of silver nanoparticle (AgNPs) on catheter surface. The formed coating was intensively characterized using spectroscopic and microscopic techniques. The coated catheter has the potential to release silver ion in a sustained manner with a concentration of about $2\text{--}4\ \mu\text{g ml}^{-1}$. Disk diffusion test and colony forming unites assay verified the significant bactericidal potential of the AgNPs coated catheter against both gram-positive and gram-negative bacteria as a consequence of silver ion release. In contrast to commercial catheter, the AgNPs coated catheter prevented the adherence of bacterial cells and biofilm formation on their surfaces. Interestingly, scanning electron microscope investigations showed that AgNPs coated catheter possess greater antifouling potential against gram-positive bacteria than against gram-negative bacteria. Overall, the remarkable antibacterial and antifouling potential of the coated catheter supported the use of such facile approach for coating of different medical devices for the prevention of nosocomial infections.

1. Introduction

Bacterial biofilm formation is a serious threat for the global economy and public health. Biofilm can be observed on various surfaces starting from plaque on teeth through food packaging materials to medical devices, water purification filters, oil pipelines and ship hulls [1]. Particularly, indwelling urinary catheters are widely used in the medical sector to assist people who can not urinate on their own. Statistics reveals that around 15%–25% of hospitalized patients receive urinary catheters during their hospital stay [2]. Urinary catheters are usually based on flexible hydrophobic polymeric materials such as silicon rubber or polyurethane, however such materials are considered as breeding surface for uropathogens to adhere to the catheter surface followed by colonization and biofilm formation [3, 4]. This in turn causes catheter-associated urinary tract infections (CAUTIs), which represent around 40 % of nosocomial infections worldwide [5]. The threat of the biofilm lay on its ability to produced extracellular polymeric substances (EPS)

consisting of polysaccharides, nucleic acids and proteins, which provides protection for the bacteria from antibiotics and human immune system [6]. Therefore, bacteria in biofilms possess high resistance towards conventional antibiotic up to 1000 fold compared to planktonic bacteria [7]. *Escherichia coli*, *Proteus mirabilis* and *Klebsiella pneumoniae* are the frequently Gram-negative bacteria associated with CAUTIs, while the Gram-positive bacteria include *Staphylococcus aureus* and *Staphylococcus epidermidis* [8].

In this context, strenuous efforts have been directed to minimize the accumulation of bacteria on the surface of urinary catheters. Generally, surface modification of catheters is often fall under one of three concepts: biopassive surfaces, bioactive surfaces or a combination of both [9]. Particularly, biopassive coating is achieved by coating the surface with hydrophilic well-hydrated polymers including poly(ethylene glycol) (PEG) or poly(2-methyl-2-oxazoline) that have the potential to prevent the adhesion of bacteria without killing them [10, 11]. In contrast, the bioactive coatings can be attained through two approaches. The first is to

* Corresponding author.

E-mail address: yassin@daad-alumni.de (M.A. Yassin).

decorate the surface with quaternary ammonium polymers that interfere with the bacteria cell wall leading to cell lysis and death [12, 13, 14]. However, the second approach relies on loading the surface with biocidal agents such as antibiotic, antiseptic, enzymes or metallic nanoparticles that under go slow release to the near surroundings causing bacterial death [15, 16, 17, 18].

Among the metal nanoparticles, silver nanoparticles (AgNPs) have been widely reported as a potential antimicrobial agent against a broad spectrum of bacterial and fungal species including the drug resistant strains [19]. Indeed, many reports demonstrated AgNPs as potential antimicrobial coating for diverse surfaces including catheters, titanium implant, textile, water membrane [20, 21, 22, 23]. Such surfaces have been decorated with AgNPs using different methods such as chemical deposition, photo-chemical deposition, physical vapor deposition and sputtering deposition techniques [21]. However, in situ formation of AgNPs is a simple and versatile strategy that is widely used to overcome the complicated multi-steps procedures that limited many applications [24, 25, 26].

Recently, several studies have explored the potential of the mussel bio-inspired dopamine to undergo self-polymerization under mild conditions forming polydopamine (PDA) [27]. Indeed, polydopamine possesses highly adhesion capacity on not only inorganic surfaces such as silica and magnetic nanoparticles but also on organic surfaces such as polymeric matrices and fabrics [28, 29, 30, 31, 32]. The adhesion force of PDA is derived from its catechol groups that form hydrogen bonding with the coated surfaces. In addition, PDA has a reductive capacity which allows the in situ metal deposition upon exposure to noble metal salt solutions [27]. In this context, PDA was reported as a facile coating for urinary catheters that acts as an active platform to attach different antimicrobial agents such as multi-layers AgNPs coated with antifouling outer layer, peptides and quaternary ammonium polymers [24, 33, 34].

Consequently, this work aims to modify the commercially available silicon urinary catheter with AgNPs as antimicrobial coating to prevent the CAUTIs. This was simply achieved using a facile approach by coating the urinary catheter with a polydopamine layer followed by deposition of AgNPs on the catheter via the in situ reduction. The coated catheters were full characterized with ATR-FTIR, scanning electron microscope. Further more intensive biological investigations have been carried out to evaluate the antimicrobial and the antifouling capacity of the PDA/AgNPs coated catheters.

2. Experimental

2.1. Materials

Dopamine hydrochloride and silver nitrate were purchased from Acros. Tris hydrochloride was obtained from molekula. Commercial foley balloon catheter (100% silicone) based on polydimethylsiloxane was purchased from Kosan Angel. Luria-Bertani (LB) medium was supplied from sigma. Other chemicals were of analytical grade.

2.2. Methods

2.2.1. Coating catheter with polydopamine/AgNPs

Catheter was cut into small pieces of two cm length and sonicated in ethanol and water for 10 min respectively then dried with a stream of nitrogen gas. Catheter pieces were incubated in a dopamine solution (2 mg ml⁻¹, 10 mm Tris, pH 8.6) under shaking at room temperature. After 24 h, catheter pieces were rinsed with distilled water for three times and dried with a stream of nitrogen gas. The polydopamine coated catheters were further treated with silver nitrate solutions with two different concentrations (5 and 10 mg ml⁻¹) for 24 h at room temperature. Finally, treated catheters were rinsed with distilled water and dried with nitrogen gas.

2.2.2. Surface characterization

ATR-FTIR spectroscopy analysis (JASCO instrument) was used to characterize the chemical composition of the pristine and coated catheters. Samples were scanned at resolution of 4 cm⁻¹ over a wavenumber range of 400–4000 cm⁻¹. The morphology of the pristine and coated catheters was investigated by scanning electron microscope (SEM, JEOL JSM-5500LV SEM, Japan). All samples were sputter-coated with thin gold layers before investigation. Energy-dispersive X-ray spectroscopy (EDX) measurements were conducted to detect Ag atom on the surface of the modified catheter.

2.2.3. Silver release determination

The DOPA/AgNPs coated catheters were incubated in 5 ml of phosphate buffered solution (pH 7.5) at 37 °C. The buffer solution was collected and replaced with fresh buffer solution at different times. The amounts of released silver were quantitatively determined by inductively coupled plasma mass spectrometry (ICP-MS, Agilent 7700X, Australia).

2.2.4. Antibacterial investigations

Gram-positive *Staphylococcus aureus* (*S. aureus*) and Gram-negative *Escherichia coli* (*E. coli*) were selected for antibacterial experiments. Pieces of the pristine commercial catheters, dopamine coated catheters and PDA/AgNPs coated catheters were placed in 24-well plates and sterilized with UV radiation (wavelength of 254 nm) for 10 min. Supposedly, the bactericidal effect of the AgNPs in situ formed on the PDA coated catheters will be due to either direct contact with bacteria or due to the release of silver ions around the bacterial species. Therefore, multiple antibacterial activity tests were performed to investigate both effects. Particularly, agar diffusion method was performed by firstly inoculating both bacterial species on solid agar plates then the catheter specimens were placed on thin layer of bacteria. The plates were incubated at 37 °C for 24 h and the growth of inhibition zones around each sample was calculated and the zones were digitally photographed.

The bactericidal potential of the PDA/AgNPs coated catheter on the viability of the bacteria suspension was quantitatively investigated using colony forming unit test. Particularly, overnight bacterial culture of both species were diluted to 1:100 in fresh sterilized Luria-Bertani (LB) medium and placed in a shaker incubator for 3–6 h until the O.D. of the bacteria at 600 nm reached about 0.8. Catheter samples were covered with 1 ml of the previous bacterial suspension and incubated overnight at 37 °C. The catheters were gently removed from the suspension with a forceps. The optical density at 600 nm of the supernatant was recorded using a spectrophotometer to show the effect of silver ions release on the viability of the bacteria suspended in the medium. The colony forming unit (CFU per mL) was calculated based on predetermined standard curves of bacteria density versus optical density at 600 nm.

To evaluate the antifouling potential of the PDA/AgNPs coated catheter, the incubated catheter was gently removed from the bacteria suspension and washed by dipping in fresh sterilized LB medium three times. To detach the adhered bacteria, the catheters were placed in 1 ml of LB medium and ultrasonically treated for 5 min. Thereafter, 0.5 ml of the LB medium was inoculated on agar plates and the viable bacterial colonies was documented by digital camera.

Finally, the effect of AgNPs on the morphology of bacteria seeded on the catheters was inspected by scanning electron microscope (SEM, JEOL JSM-5500LV SEM, Japan). Both gram positive and gram negative bacteria were separately seeded on the pristine and coated catheters and left overnight at 37 °C. The samples were rinsed with distilled water and fixed with 2.5 % glutaraldehyde overnight at 4 °C, then the fixed bacteria was dehydrated in graded ethanol series (30, 50, 75, 90, 95 and 100 v/v %). Subsequently, the samples were sputter-coated with thin gold layers for observation by SEM. Energy-dispersive X-ray spectroscopy (EDX) measurements were conducted to show Ag atom on the surface of the catheter.

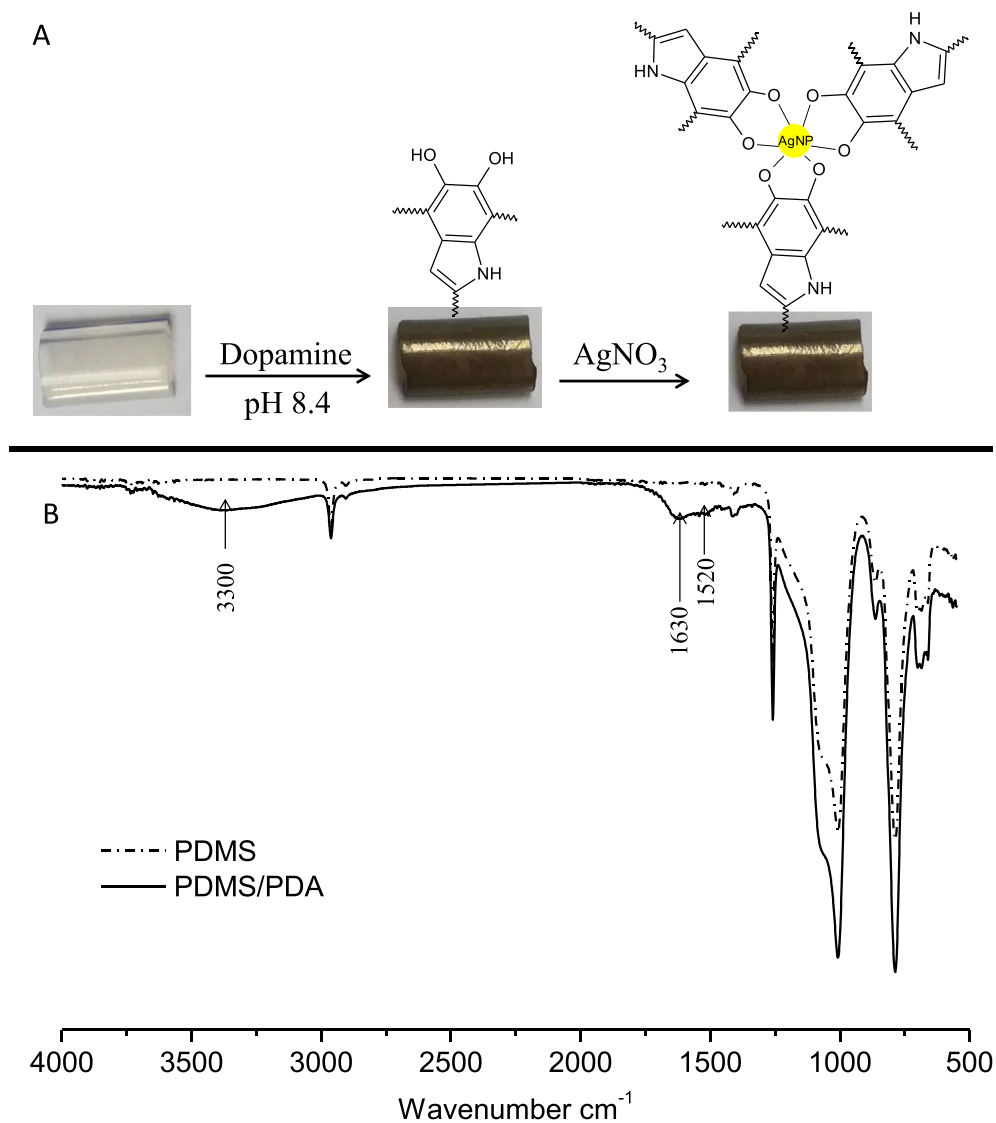


Figure 1. A) Photographic image of catheter at the different modification steps, B) ATR-FTIR analysis of pristine catheter (PDMS) and PDA coated catheter.

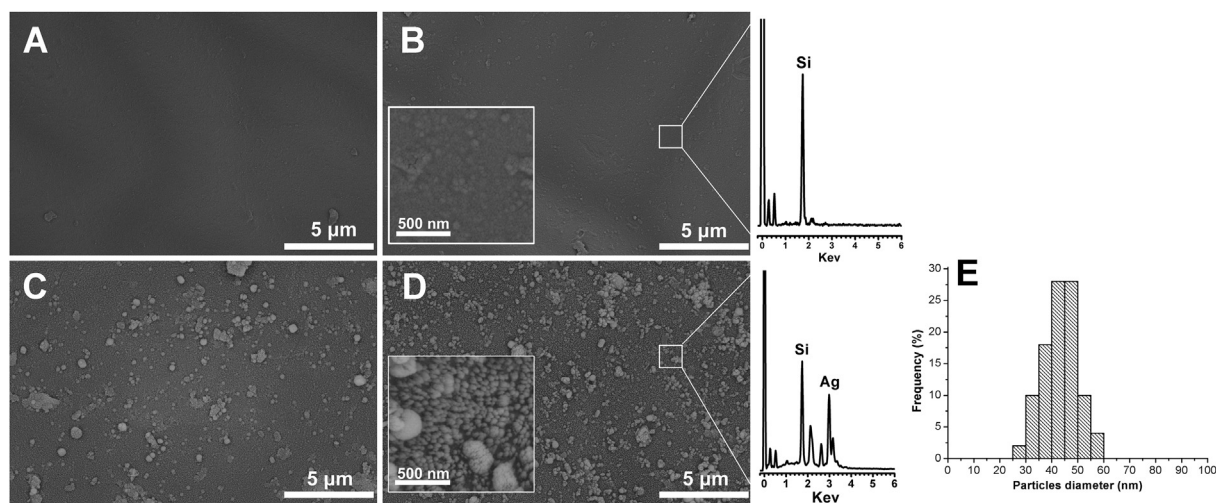


Figure 2. SEM images show the morphology of pristine catheter (A), PDA coated catheter (B), PDA/AgNPs coated catheters at 5 and 10 mg ml⁻¹ of AgNO₃ (C and D). Mean particle diameter of AgNPs (E). The inset images represent the same sample at higher magnification and EDX analysis represents PDA and PDA/AgNPs coated catheters.

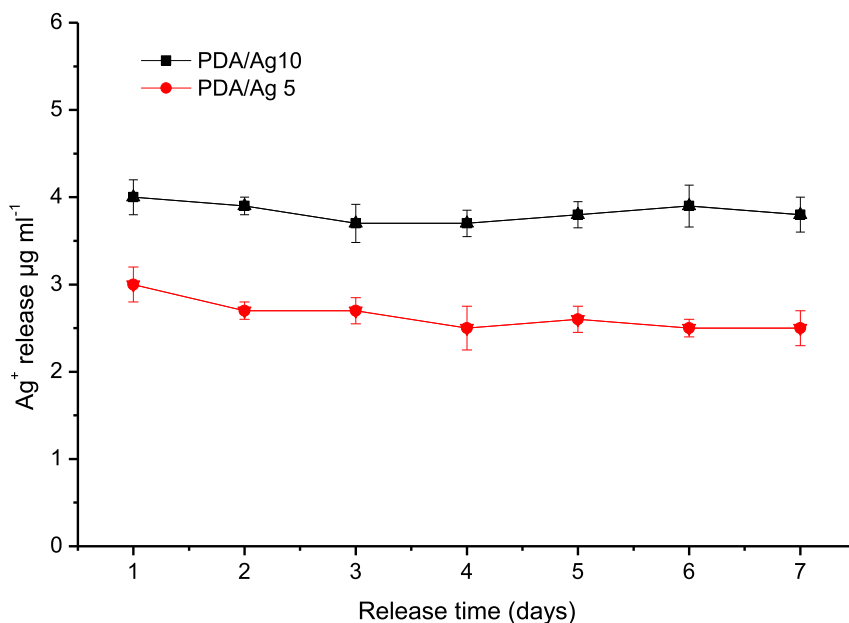


Figure 3. Time-dependent Ag⁺ release from the PDA/AgNPs coated catheter prepared at different concentrations of AgNO₃, 5 mg ml⁻¹ (PDA/Ag 5) and 10 mg ml⁻¹ (PDA/Ag 5). Investigations carried out at 37 °C in phosphate buffer pH 7.5.

3. Results and discussion

The silicon urinary catheter was initially coated with a layer of the bio-inspired polydopamine (PDA) by simple dip coating in dopamine solution in alkaline pH for 24 h. It was obviously observed that the color of catheter was turned from transparent to brown indicating the formation of polydopamine layer on the catheter (Figure 1A). This was further confirmed by ATR-FTIR spectroscopy as depicted in Figure 1B. The pristine catheter showed the characteristic bands of polydimethylsiloxane (PDMS) at 1040 cm⁻¹ and 780 cm⁻¹ corresponding to the O-Si-O and Si-CH₃, respectively [35]. However, the polydopamine coated catheter displayed new broad absorption band at 3300 cm⁻¹ that correspond to the stretching vibrations of -OH and N-H groups of the PDA. Moreover, peak at 1630 cm⁻¹ is assignable to the carbonyl groups and peak at 1520 cm⁻¹ is assignable to C=N and C=C of PDA [36].

The next step was to use the formed PDA layer as an active platform to deposit AgNPs on the PDA coated catheter using the innate reductive capacity of PDA, which allows the in situ silver metal deposition upon exposure to silver nitrate solutions [27]. This phenomenon is attributable to the redox reactions between residual catechol groups of PDA layer and

Ag⁺ ions, forming Ag⁰ at the solid liquid interface (Figure 1A). To achieve this, the dopamine coated catheters were inculcated into solution of silver nitrate at different concentrations (5 and 10 mg ml⁻¹) for 24 h. As depicted in Figure 2, Scanning Electron Microscope was used to investigate the surface morphology of the pristine catheter, PDA coated catheter and PDA/AgNPs coated catheters. The pristine catheter showed a smooth surface (Figure 2A). After incubation with dopamine, a layer of the self-polymerized polydopamine was observed (Figure 2B) which appeared in the higher magnification as individual or aggregated PDA particles. The catheters morphology was obviously altered after dipping into different concentrations of AgNO₃ solutions. Figure 2C and D showed the formation of AgNPs on the PDA coated catheters treated with 5 and 10 mg ml⁻¹ of AgNO₃, respectively. It was obvious that the density of AgNPs was increased by increasing the concentration of AgNO₃. The AgNPs displayed an average size of about 30–50 nm (Figure 2E), however sup-micron agglomerations on top of the nano-sized AgNPs in the base layer were observed as well. Additionally, the Energy-dispersive X-ray spectroscopy (EDX) of the PDA and PDA/AgNPs coated catheters further confirmed that the formed nanoparticles are related to silver nanoparticles.

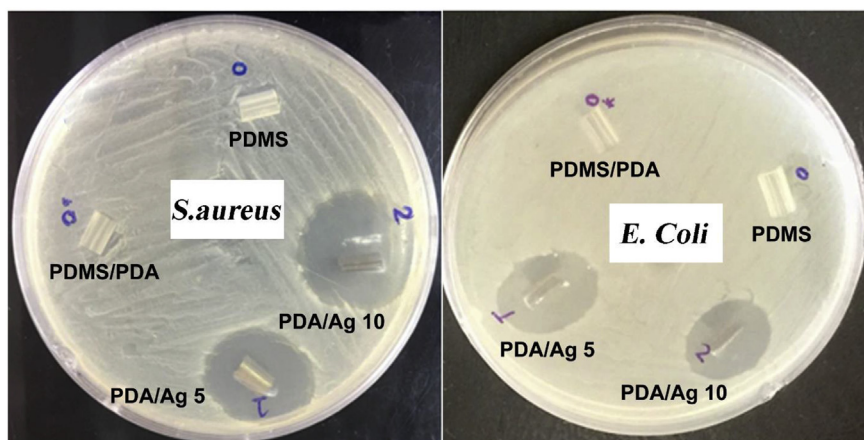


Figure 4. Inhibition zone assay of pristine silicone catheter (PDMS), catheter coated with polydopamine layer (PDMS/PDA) and catheter coated with polydopamine and then incubated with different concentrations of AgNO₃; 5 mg ml⁻¹ (PDA/Ag 5) and 10 mg ml⁻¹ (PDA/Ag 10) for 24 h.

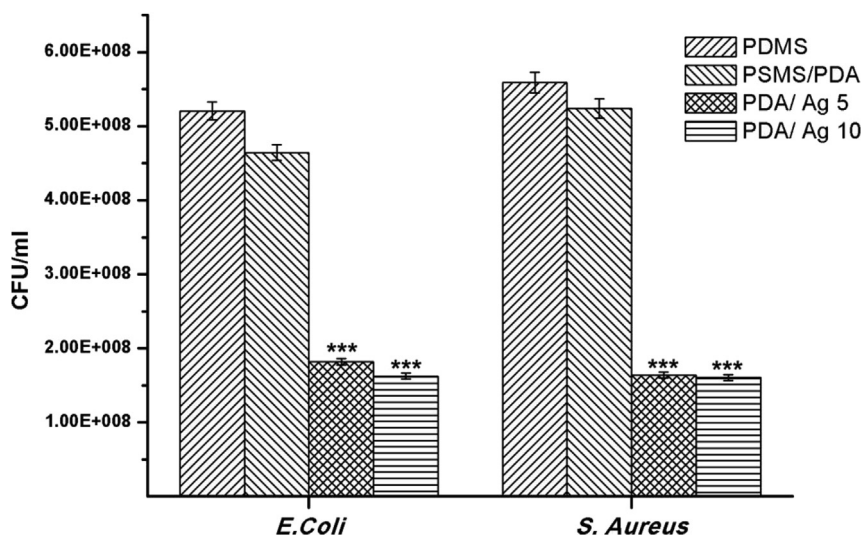


Figure 5. Colonies forming unit (CFU) of *S. aureus* and *E. coli* after incubation for 24 h with pristine catheter (PDMS), PDA coated catheter (PDMS/PDA) and PDA/AgNPs coated catheters at 5 (PDA/Ag 5) and 10 mg ml⁻¹ (PDA/Ag 10) silver nitrate, respectively. (***)p < 0.001).

Since the antibacterial activity of AgNPs coated catheter is dependent on the release of silver ions, time-dependent Ag⁺ release from the PDA/AgNPs coated catheter was investigated at 37 °C using ICP analysis. Figure 3 illustrated that silver was released in a sustained manner with constant rate during the first seven days [37, 38]. The release rate was dependent on the density of AgNPs where a higher amount of Ag⁺ was released from catheter treated with 10 mg ml⁻¹ of AgNO₃ (PDA/Ag 10) compared with that treated with 5 mg ml⁻¹ of AgNO₃ (PDA/Ag 5). Generally, the amount of Ag⁺ released from the treated catheter was about 2–4 μg ml⁻¹. Such silver concentration is higher than the minimal biocidal concentration (1.5 μg ml⁻¹) and less than 10 μg ml⁻¹ that is considered as a toxic concentration to human cells [24, 39].

The Kirby–Bauer disc diffusion test was used to evaluate the bactericidal efficiency of AgNPs deposited on PDA coated catheter. Figure 4 shows the inhibition zones of PDA/AgNPs coated catheters as compared to the pristine and PDA coated catheters against *S. aureus* and *E. coli*. The surface of pristine and PDA coated catheters did not exhibit inhibition zone indicating the lack of bactericidal activity of the commercial and PDA coated catheters. However, catheters coated with AgNPs at different silver nitrate concentrations displayed remarkable bactericidal activities

against both gram positive and gram negative bacteria. Particularly, gram negative strain (*E. coli*) showed clear inhibition zones with diameter of 19 and 18.5 mm for PDA/Ag 5 and PDA/Ag 10, respectively. While, PDA/Ag 5 and PDA/Ag 10 recorded inhibition zones against gram positive strain (*S. aureus*) with diameters of 23 and 26 mm, respectively.

The lethal effect of AgNPs to wide spectrum of pathogenic bacterial strains is derived from two possibilities. The first is the direct contact of AgNPs with the cell membrane of attached bacterial leading to pits formation which in turn lead to permeability loss and cell death [40]. The other possibility is the release of silver ions from AgNPs which interact with the thiol groups in protein leading to protein deactivation and death of both attached and swimming bacteria [25]. To evaluate the influence of the released silver ions from the coated catheter on the swimming bacteria, the O.D. of LB medium (supernatant) was measured after 24 h of incubation with pristine and modified catheters and then converted to CFU by using standard curves (CFU vs O.D.) for both bacterial strains. Figure 5 clearly displayed that the number of live bacteria in the growth medium was drastically reduced after incubation with PDA/AgNPs catheters as compared to PDMS and PDMS/PDA catheters. Indeed, PDA/AgNPs coated catheter possesses similar bactericidal potential

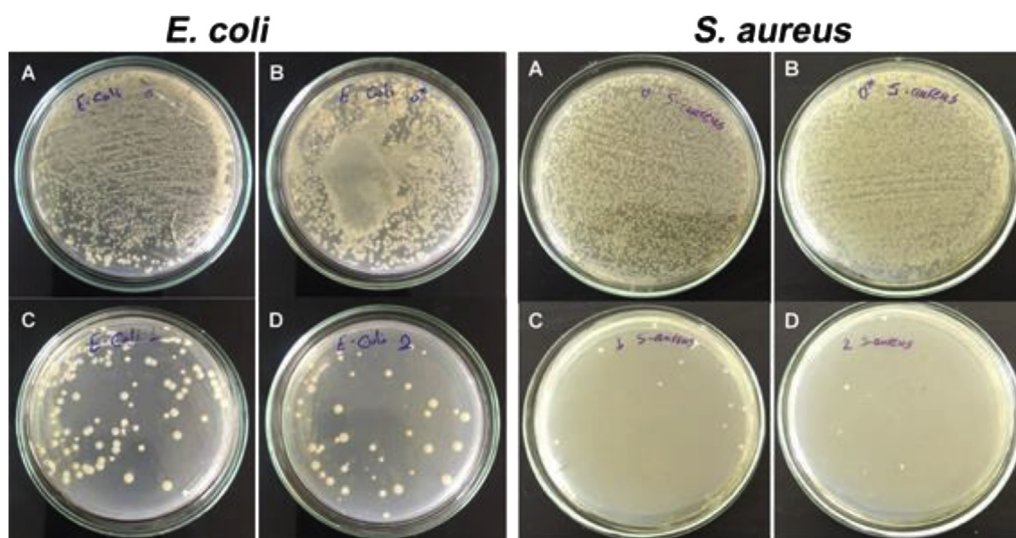


Figure 6. Digital images of two bacteria strains which were detached from the surface of PDMS (A), PDMS/PDA (B), PDA/Ag 5 (C) and PDA/Ag 10 (D) and re-inoculated on agar plates showing only the viable bacterial colonies that remained adhered on the surface after 24 h of incubation.

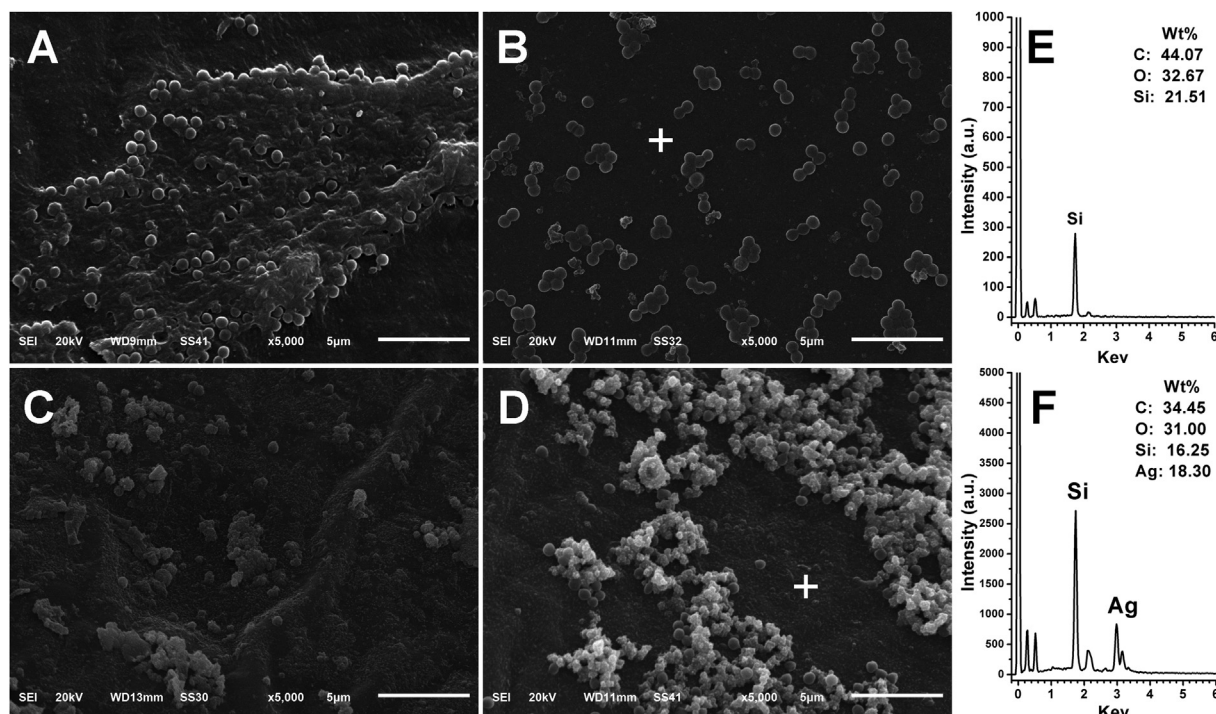


Figure 7. Low magnification SEM images (5000 x) of spherical-shaped *S. aureus* grown onto different surfaces for 24 h. (A) PDMS, (B) PDMS/PDA, (C) PDA/Ag 5 and (D) PDA/Ag 10. EDX spectra of the base layers on the surface of samples PDMS/PDA (E) and PDMS/PDA 10 (F); the scanned spot represented by white plus mark (+) on both images B and D.

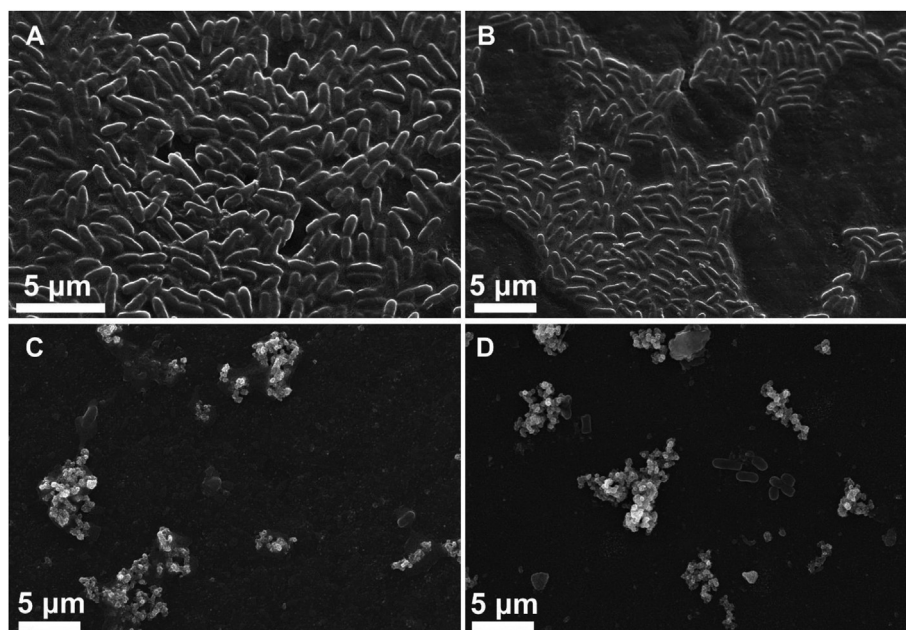


Figure 8. Low magnification SEM images (5000 x) of rod-shaped *E. coli* grown onto different surfaces for 24 h. (A) PDMS, (B) PDMS/PDA, (C) PDA/Ag 5 and (D) PDA/Ag 10.

against the non-adherent (swimming) bacteria of both *S. aureus* and *E. Coli*.

To evaluate the antifouling potential of the PDA/AgNPs coated catheter, spread plate method was conducted to count the viable bacteria colonies that remained adhered on the surface of pristine and modified catheters. As shown in Figure 6, pristine and PDA coated catheters showed high number of viable colonies of both strains indicating the high accumulation and adherence of bacteria on catheter surfaces. However,

the numbers of viable colonies accumulated on the surface of silver coated catheter were far less compared to the pristine and PDA coated catheters. It was obvious from spread plate test (Figure 6) that the antifouling potential of silver coated catheter was greater against gram positive than against gram negative bacteria. This is attributed to the fact that the cell walls of gram positive bacteria bind larger quantities of metals than gram negative bacteria which in turn leads to higher bactericidal potential and less living bacteria attached on surface [40].

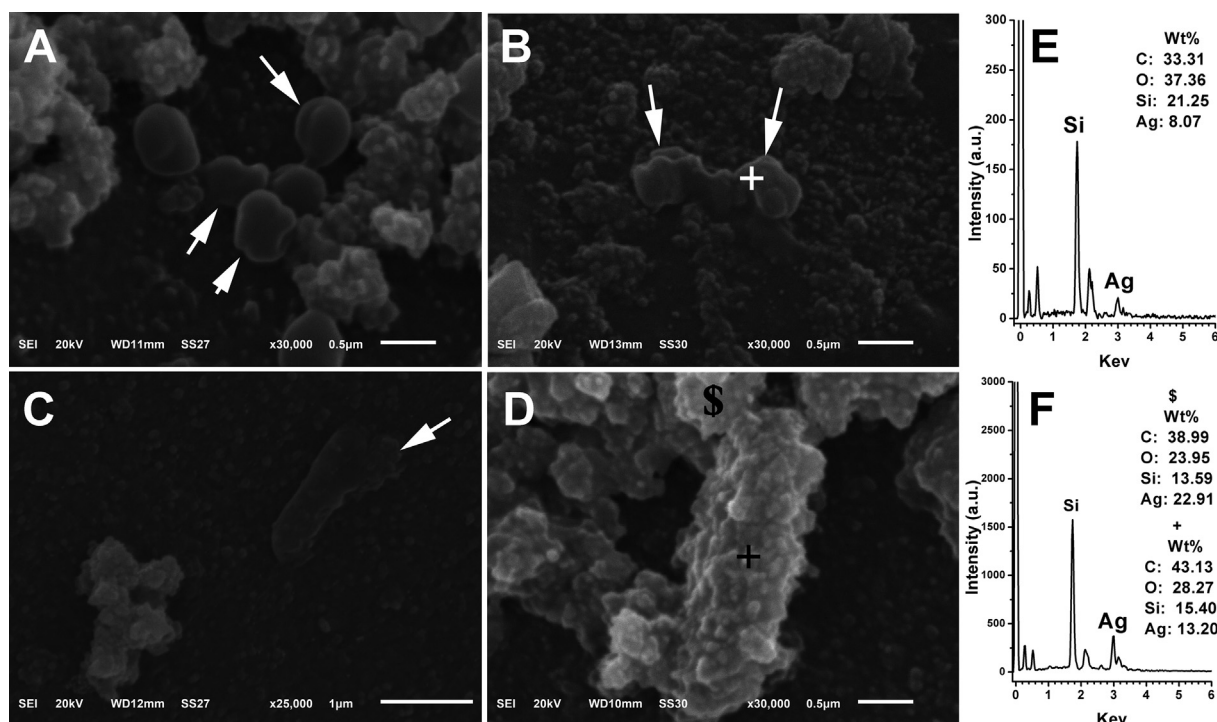


Figure 9. High magnification SEM images of *S. aureus* (A and B) and *E. coli* (C and D) grown onto sample PDA/Ag 10 for 24 h. EDX spectra and weight percentage of the elements on figures E and F represent the sign (+ and \$) on images B and D, respectively.

Morphological studies of both bacterial strains on unmodified and modified catheter surfaces was monitored by SEM and complementary EDX spectra was acquired for elemental surface analysis as shown in Figures 7 and 8. On the surface of pristine catheter, it is clearly shown in Figure 7A that the grape-shaped *S. aureus* are embedded in an extracellular matrix (biofilm) and the morphology of the cells is intact, suggesting that the surface of the commercial catheter is prone to bacteria proliferation and subsequent infection. On PDMS/PDA surface, the bacteria formed groups of small colonies, however there was no sign of biofilm formation (Figure 7B). On contrary, Figure 7C and D showed that number of bacteria was significantly reduced on the surface of silver coated catheters, suggesting that AgNPs based coatings could inhibit bacteria adhesion and biofilm formation. In case of using high concentration of AgNO_3 (PDA/Ag 10), there was a higher propensity for the formation of micron-sized agglomeration on top of the nano-sized AgNPs in the base layer. In Figure 7D, it can be seen that *S. aureus* are dispersed within these large clusters of AgNPs which proves that bacteria can be directly attached to surface of AgNPs but they suffer deformation in their morphology due to this direct contact. The EDX spectra in Figure 7E and F revealed the lack of silver peak in case of PDMS/PDA surface and the presence of silver peak on base layer away from the agglomerates proving that the surface coated with silver consists of base layer with nano-sized AgNPs and silver clusters with sub-micron size.

Additionally, the morphology of rod-shaped *E. Coli* seeded on all different surfaces was inspected by SEM as shown in Figure 8. High density of smooth *E. Coli* with sound cell membrane and embedded in biofilm matrix were observed on the commercial catheter (PDMS) and PDMS/PDA catheter. However, silver coated catheters displayed a significant decrease in number of *E. coli* with irregular morphology and rougher surface.

The lethal effect of AgNPs on shape deformation of both *S. aureus* and *E. Coli* was explained from the high magnification SEM micrographs in Figure 9. It is well reported that the dissolution of AgNPs due to oxidation process results in release of Ag^+ ions in the surrounding environment of the bacteria [24]. These ions interact and accumulate on the cell membrane of the bacteria leading to rupture of cell membrane and

subsequently leakage of the cytosolic components [25]. In Figure 9A and B, it is clearly shown that the morphology of rounded *S. aureus* is severely deformed (indicated by white arrows) due to the formation of longitudinal clefts and pits which lead to leakage of cytoplasm and eventually shrinkage of bacteria. Bacterial cell lysis was also observed due to direct contact with AgNPs as shown in Figure 9C. To prove the involvement of Ag species in the deformation of bacteria cell morphology, EDX spectra (spot scan indicated by + sign) were recorded on the surface of both *S. aureus* and *E. Coli* as shown in Figure 9E and F, respectively. It can be seen that silver peaks were detected on the bacteria surface which indicate the interaction between bacteria surface and silver which can cause membrane lysis and fragmentation of bacterial cells.

Overall, the low number of bacteria along with deformed morphological appearance indicated that coating catheter with bio-inspired polydopamine layer and the utilization of its self-reducing capacity to form AgNPs is a facile strategy to establish antifouling and bactericidal coating on silicone based urinary catheter.

4. Conclusion

Commercial urinary catheter based on silicon rubber was coated with silver nanoparticles using facile approach to impart antifouling and antibacterial properties on the coated catheters. Particularly, catheter was simply dip coated with a layer of bio-inspired polydopamine which acts as active platform for the in situ formation of AgNPs. ATR-FTIR and SEM analysis confirmed the successful coating with PDA and the formed AgNPs have average size of 30–50 nm however, sub-micron clusters were observed as well. The amount of silver ions released from the catheter was about $2\text{--}4 \mu\text{g ml}^{-1}$ which is less than $10 \mu\text{g ml}^{-1}$ that is considered as a toxic concentration to human cell. Agar diffusion test, CFU and intensive SEM investigations proved that AgNPs coated catheter possess remarkable bactericidal activity against both gram positive and gram negative bacteria. However, gram positive bacteria were more susceptible to AgNPs than gram negative bacteria. Furthermore, the coated catheter displayed outstanding potential to prevent the fouling of both bacteria strains as compared to the commercial catheter. Accordingly,

coating catheter with bio-inspired polydopamine layer and the utilization of its self-reducing capacity to form AgNPs is a promising and fast strategy to establish antifouling and bactericidal coating on silicone based medical devices.

Declarations

Author contribution statement

Mohamed A. Yassin: Conceived and designed the experiments; Performed the experiments; Analyzed and interpreted the data; Contributed reagents, materials, analysis tools or data; Wrote the paper.

Tarek A. Elkhooly: Conceived and designed the experiments; Performed the experiments; Analyzed and interpreted the data; Wrote the paper.

Shereen M. Elsherbiny: Performed the experiments.

Fikry M. Reicha: Analyzed and interpreted the data.

Ahmed A. Shokeir: Conceived and designed the experiments; Analyzed and interpreted the data.

Funding statement

This work was financially supported through a competitive project funded by Mansoura University.

Competing interest statement

The authors declare no conflict of interest.

Additional information

No additional information is available for this paper.

References

- [1] P. Zou, W. Hartleb, K. Lienkamp, It takes walls and knights to defend a castle – synthesis of surface coatings from antimicrobial and antibiofouling polymers, *J. Mater. Chem.* 22 (2012) 19579–19589.
- [2] Z. Zhu, Z. Wang, S. Li, X. Yuan, Antimicrobial strategies for urinary catheters, *J. Biomed. Mater. Res. A* 107 (2019) 445–467.
- [3] H. Wang, F. Teng, X. Yang, X. Guo, J. Tu, C. Zhang, et al., Preventing microbial biofilms on catheter tubes using ultrasonic guided waves, *Sci. Rep.* 7 (2017) 616.
- [4] S. Anjum, S. Singh, L. Benedicte, P. Roger, M. Panigrahi, B. Gupta, Biomodification strategies for the development of antimicrobial urinary catheters: overview and advances, *Global Challenges* 2 (2018) 1700068.
- [5] C.E. Armbruster, H.L. Mobley, Merging mythology and morphology: the multifaceted lifestyle of *Proteus mirabilis*, *Nat. Rev. Microbiol.* 10 (2012) 743–754.
- [6] R. Campana, F. Biondo, F. Mastrotto, W. Baffone, L. Casetari, Chitosans as new tools against biofilms formation on the surface of silicone urinary catheters, *Int. J. Biol. Macromol.* 118 (2018) 2193–2200.
- [7] S. Swar, V. Zajicová, M. Rysová, I. Lovětinská-Šlamborová, L. Voleský, I. Stibor, Biocompatible surface modification of poly(ethylene terephthalate) focused on pathogenic bacteria: promising prospects in biomedical applications, *J. Appl. Polym. Sci.* 134 (2017).
- [8] S. Niveditha, S. Pramodhini, S. Umadevi, S. Kumar, S. Stephen, The isolation and the biofilm formation of uropathogens in the patients with catheter associated urinary tract infections (UTIs), *J. Clin. Diagn. Res. : J. Clin. Diagn. Res.* 6 (2012) 1478–1482.
- [9] M. Charnley, M. Textor, C. Acikgoz, Designed polymer structures with antifouling–antimicrobial properties, *React. Funct. Polym.* 71 (2011) 329–334.
- [10] L. Bai, L. Tan, L. Chen, S. Liu, Y. Wang, Preparation and characterizations of poly(2-methyl-2-oxazoline) based antifouling coating by thermally induced immobilization, *J. Mater. Chem. B* 2 (2014) 7785–7794.
- [11] C. Diaz Blanco, A. Ortner, R. Dimitrov, A. Navarro, E. Mendoza, T. Tzanov, Building an antifouling zwitterionic coating on urinary catheters using an enzymatically triggered bottom-up approach, *ACS Appl. Mater. Interfaces* 6 (2014) 11385–11393.
- [12] X. Ding, C. Yang, T.P. Lim, L.Y. Hsu, A.C. Engler, J.L. Hedrick, et al., Antibacterial and antifouling catheter coatings using surface grafted PEG-b-cationic polycarbonate diblock copolymers, *Biomaterials* 33 (2012) 6593–6603.
- [13] M. Gultekinoglu, B. Kurum, S. Karahan, D. Kart, M. Sagioglu, N. Ertaş, et al., Polyethyleneimine brushes effectively inhibit encrustation on polyurethane ureteral stents both in dynamic bioreactor and in vivo, *Mater. Sci. Eng. C* 71 (2017) 1166–1174.
- [14] M.H. Abdel Rehim, M.A. Yassin, H. Zahran, S. Kamel, M.E. Moharam, G. Turky, Rational design of active packaging films based on polyaniline-coated polymethyl methacrylate/nanocellulose composites, *Polym. Bull.* (2019).
- [15] A. Vaterodt, B. Thallinger, K. Daumann, D. Koch, G.M. Guebitz, M. Ulbricht, Antifouling and antibacterial multifunctional polyzwitterion/enzyme coating on silicone catheter material prepared by electrostatic layer-by-layer assembly, *Langmuir* 32 (2016) 1347–1359.
- [16] S. Srisang, N. Nasongkla, Layer-by-layer dip coating of Foley urinary catheters by chlorhexidine-loaded micelles, *J. Drug Deliv. Sci. Technol.* 49 (2019) 235–242.
- [17] M. Stenger, K. Klein, R.B. Grønnemose, J.K. Klitgaard, H.J. Kolmos, J.S. Lindholt, et al., Co-release of dicloxacillin and thioridazine from catheter material containing an interpenetrating polymer network for inhibiting device-associated *Staphylococcus aureus* infection, *J. Control. Release* 241 (2016) 125–134.
- [18] Y. Shalom, I. Perelshtein, N. Perkas, A. Gedanken, E. Banin, Catheters coated with Zn-doped CuO nanoparticles delay the onset of catheter-associated urinary tract infections, *Nano Res.* 10 (2017) 520–533.
- [19] S. Tang, J. Zheng, Antibacterial activity of silver nanoparticles: structural effects, *Adv. Healthc. Mater.* 7 (2018) 1701503.
- [20] M.S. Haider, G.N. Shao, S.M. Imran, S.S. Park, N. Abbas, M.S. Tahir, et al., Aminated polyethersulfone-silver nanoparticles (AgNPs-APES) composite membranes with controlled silver ion release for antibacterial and water treatment applications, *Mater. Sci. Eng. C* 62 (2016) 732–745.
- [21] J. Wang, Z. Li, Y. Liang, S. Zhu, Z. Cui, H. Bao, et al., Cytotoxicity and antibacterial efficacy of silver nanoparticles deposited onto dopamine-functionalised titanium, *Mater. Exp.* 5 (2015) 191–200.
- [22] M.A. Syed, S. Babar, A.S. Bhatti, H. Bokhari, Antibacterial effects of silver nanoparticles on the bacterial strains isolated from catheterized urinary tract infection cases, *J. Biomed. Nanotechnol.* 5 (2009) 209–214.
- [23] H.B. Ahmed, H.E. Emam, H.M. Mashaly, M. Rehan, Nanosilver leverage on reactive dyeing of cellulose fibers: color shading, color fastness and biocidal potentials, *Carbohydr. Polym.* 186 (2018) 310–320.
- [24] R. Wang, K.G. Neoh, E.T. Kang, P.A. Tambyah, E. Chiong, Antifouling coating with controllable and sustained silver release for long-term inhibition of infection and encrustation in urinary catheters, *J. Biomed. Mater. Res. B Appl. Biomater.* 103 (2015) 519–528.
- [25] M.L. Kung, P.Y. Lin, S.W. Peng, D.C. Wu, W.J. Wu, B.W. Yeh, et al., Biomimetic polymer-based Ag nanocomposites as an antimicrobial platform, *Appl. Mater. Today* 4 (2016) 31–39.
- [26] H.E. Emam, Arabic gum as bio-synthesizer for Ag–Au bimetallic nanocomposite using seed-mediated growth technique and its biological efficacy, *J. Polym. Environ.* 27 (2018) 210–223.
- [27] Y. Liu, K. Ai, L. Lu, Polydopamine and its derivative materials: synthesis and promising applications in energy, environmental, and biomedical fields, *Chem. Rev.* 114 (2014) 5057–5115.
- [28] T.A. Elkhooly, W.E.G. Müller, X. Wang, W. Tremel, S. Isbert, M. Wiens, Bioinspired self-assembly of tyrosinase-modified silicatein and fluorescent core–shell silica spheres, *Bioinspiration Biomim.* 9 (2014), 044001.
- [29] M. Martín, P. Salazar, R. Villalonga, S. Campuzano, J.M. Pingarrón, J.L. González-Mora, Preparation of core–shell Fe₃O₄@poly(dopamine) magnetic nanoparticles for biosensor construction, *J. Mater. Chem. B* 2 (2014) 739–746.
- [30] H. Niu, S. Wang, T. Zeng, Y. Wang, X. Zhang, Z. Meng, et al., Preparation and characterization of layer-by-layer assembly of thiols/Ag nanoparticles/polydopamine on PET bottles for the enrichment of organic pollutants from water samples, *J. Mater. Chem.* 22 (2012) 15644.
- [31] Z. Xu, K. Miyazaki, T. Hori, Fabrication of polydopamine-coated superhydrophobic fabrics for oil/water separation and self-cleaning, *Appl. Surf. Sci.* 370 (2016) 243–251.
- [32] M. Yassin, M. Naguib, M. Abdel Rehim, K. Ali, Immobilization of β -galactosidase on carrageenan gel via bio-inspired polydopamine coating, *J. Text. Col. Polym. Sci.* 0 (2018) 0.
- [33] K. Lim, R.R. Chua, H. Bow, P.A. Tambyah, K. Hadinoto, S.S. Leong, Development of a catheter functionalized by a polydopamine peptide coating with antimicrobial and antibiofilm properties, *Acta Biomater.* 15 (2015) 127–138.
- [34] V.C. Thompson, P.J. Adamson, J. Dilag, DB Uswatte Uswatte Lianage, K. Srikantharajah, A. Blok, et al., Biocompatible anti-microbial coatings for urinary catheters, *RSC Adv.* 6 (2016) 53303–53309.
- [35] J. Yang, Q. Zhou, K. Shen, N. Song, L. Ni, Controlling nanodomain morphology of epoxy thermosets templated by poly(caprolactone)-block-poly(dimethylsiloxane)-block-poly(caprolactone) ABA triblock copolymer, *RSC Adv.* 8 (2018) 3705–3715.
- [36] H. Luo, C. Gu, W. Zheng, F. Dai, X. Wang, Z. Zheng, Facile synthesis of novel size-controlled antibacterial hybrid spheres using silver nanoparticles loaded with polydopamine spheres, *RSC Adv.* 5 (2015) 13470–13477.
- [37] X. Liu, J. Chen, C. Qu, G. Bo, L. Jiang, H. Zhao, et al., A mussel-inspired facile method to prepare multilayer-AgNP-loaded contact lens for early treatment of bacterial and fungal keratitis, *ACS Biomater. Sci. Eng.* 4 (2018) 1568–1579.
- [38] T.S. Sileika, H.D. Kim, P. Maniak, P.B. Messersmith, Antibacterial performance of polydopamine-modified polymer surfaces containing passive and active components, *ACS Appl. Mater. Interfaces* 3 (2011) 4602–4610.
- [39] Z.J. Guo, C. Chen, Q. Gao, Y.B. Li, L. Zhang, Fabrication of silver-incorporated TiO₂ nanotubes and evaluation on its antibacterial activity, *Mater. Lett.* 137 (2014) 464–467.
- [40] T.A. Abalkhil, S.A. Alharbi, S.H. Salmen, M. Wainwright, Bactericidal activity of biosynthesized silver nanoparticles against human pathogenic bacteria, *Biotechnol. Equip.* 31 (2017) 411–417.